An Adaptive Basis Function Solution to the 1D and 2D Inverse Scattering Problems using the DBIM and the BIM

Ian Jeffrey, Vladimir I. Okhmatovski, Joe LoVetri, and Colin Gilmore

Department of Electrical and Computer Engineering
University of Manitoba, Winnipeg, MB, R3T 5V6, Canada
ijeffrey@ee.umanitoba.ca, okhmatov@ee.umanitoba.ca, lovetri@ee.umanitoba.ca

Abstract**—**We present the use of an adaptive set of basis functions used in conjunction with the MoM to solve the linearized scalar inverse electromagnetic scattering problem. The basis functions, which are whole-domain and harmonic, are selected to provide a perfectly conditioned solution under the first-order Born approximation when multiple frequency experiments are considered. In order to iteratively solve the full non-linear problem by the Distorted Born Iterative Method (DBIM) and/or the Born Iterative Method (BIM), we introduce a single parameter into the basis function expansion to demonstrate that it is possible to maintain a well-conditioned linearized inverse problem by selecting the parameter value that minimizes the condition number of the discrete matrix operator. The proposed technique eliminates the need for Tikhonov regularization or equivalent regularization schemes commonly applied to the single-frequency, pulse-basis formulation of the linearized inverse scattering problem.

Keywords**—**Inverse imaging, Distorted Born, Born, Iterative methods, regularization.

I. INTRODUCTION

It is well documented that the continuous, non-linear, time-harmonic, scalar inverse scattering problem in electromagnetics is ill-posed [1], [2]. In fact, using monochromatic interrogation and a first-order linearizing assumption such as the Born approximation [3], the linear inverse problem results in a Fredholm integral equation of the first kind that retains the ill-posedness of the full non-linear problem. As the resulting operator has a null-space, no unique solution exists and one must select one of an infinite number of solutions by imposing additional constraints, a process known as regularization [2], [4].

It is beneficial to examine the cause of the ill-posedness of the problem in order to choose a suitable regularization technique. In the linearized inverse scattering problem, the smooth nature of the kernel tends to suppress the effects of high-frequency spatial variations of the unknown contrast function on the measured field values, thereby making the high-frequency contrast components irrecoverable from the field data [4]. Thus, a suitable regularization technique should, in some way, limit the high frequency components of the reconstructed contrast function.

A common way of solving the linearized inverse problem is to discretize the unknown contrast function in terms of a pulse basis expansion [5], [6] which, in itself, imposes no constraint on the maximum spatial frequency of the reconstructed contrast. Due to the ill-posedness of the continuous problem, the resulting discrete linear system is ill-conditioned [4] and, without regularization, directly solving the system yields a solution with little to no physical significance. Consequently, one of two types of regularization methods is commonly applied to the discrete system. The first, Tikhonov regularization, imposes a penalty constraint weighted by a regularization parameter. The parameter attempts to balance the error in the residual against the error inherent in the high spatial-frequency components [4-6]. Tikhonov regularization is capable of providing solutions that converge to the unknown contrast function when an iterative solution of the full-nonlinear problem is adopted [5], [6]. Unfortunately, the first-order approximation is often highly oscillatory depending on the type of penalty function selected (as shown in the numerical results of [5]) and gives little insight as to the physical nature of the true contrast.

The second popular regularization technique is the so-called truncated singular value decomposition method (TSVD) [4], [7]. As its name implies, this approach truncates the singular value reconstruction of the solution thereby constraining the high spatial-frequency components of the pulse-based solution. In fact, TSVD can be shown to be "*essentially equivalent to Tikhonov regularization when the penalty matrix is taken as the identity matrix*" [4]. Under this equivalence the truncation order substitutes as a regularization parameter.

While for both Tikhonov regularization and TSVD there exist mathematical methods for determining a suitable value of the regularization parameter [4], [7], the solution is often quite sensitive to the parameter value and selecting an appropriate parameter can be both difficult and computationally expensive. The tools are, however, quite powerful and in cases when one has no choice but to regularize the problem by the aforementioned methods, they enable a meaningful solution to be obtained. The inverse scattering problem does not, however, necessarily require formal regularization provided that the problem is *formulated* carefully. Our approach is to select equations that arrive at a discrete system where only a single, meaningful solution is possible. Further, we wish to choose our equations in such a way that the Born Approximation remains a meaningful first-order solution *i.e.*, it is a smooth first-order approximation to the unknown contrast.

With this in mind, we note that in special cases the Born approximation is capable of annihilating the null-space of the discrete operator giving a unique first-order solution. Specifically, under plane-wave incidence, the measured field data may be identified as the spatial Fourier Transform of the unknown contrast function [3], [8]. Therefore, by applying an inverse Fourier Transform to the field data we may uniquely obtain the contrast up to some maximum spatial-frequency, a result that is sometimes referred to as Fourier Imaging. Thus, in Fourier Imaging, it is by multiple frequency experiments that we "regularize" the problem (in so far as we manage to make the solution both physical and unique). Essentially, we are adding information. Fourier techniques also have the advantage of a smooth, first-order approximation to the unknown contrast function [2].

In this paper, based on the idea that Fourier Imaging offers a well-conditioned first-order solution, we first derive a perfectly conditioned MoM formulation of the inverse problem by expanding the contrast function in terms of whole-domain complex exponential basis functions, *i.e.*, the Fourier series harmonics. Second, as the limitations of the Born approximation are well known, we present a parameterized set of harmonic basis functions suitable for iterative solution schemes for solving the full non-linear problem such as the Born Iterative Method (BIM) [5] and the Distorted Born Iterative Method (DBIM) [9].

As the focus of this paper is to illustrate the benefits of the proposed basis function expansion, we focus primarily on applying the basis functions to the (D)BIM solutions for the simple 1D, lossless, noise-free problem which serves as a well documented benchmark for new inverse solution methods [1], [7]. To show that the theory can be extended to higher dimensions, we include a 2D formulation for the BIM. For both the 1D and 2D cases considered, we show successful reconstruction results.

What is presented herein is an elaboration of the work we have presented at various conferences during the past year [10-13]. We provide all details of the formulation and show results for both the BIM and the DBIM on the same problems.

II. The MoM Solution to the 1D Scattering Problem under the Born Approximation

Consider the 1D integral equation for electromagnetic scattering,

$$E(x) = E^{inc}(x) + k_0^2 \int_{-\infty}^{\infty} (\varepsilon(x') - 1)E(x')G(x, x')dx' \qquad (1)$$

where $E(x)$ is the transverse component of the electric field, $E^{inc}(x)$ is the incident electric field, $\varepsilon(x)$ is the unknown relative permittivity as a function of position and where k_0 is the wavenumber of free space. Throughout this paper an $e^{i\omega t}$ time dependence is suppressed where $i = \sqrt{-1}$ and ω is the radial frequency of the electric field. The free-space Green's function $G(x, x')$ is,

$$G(x, x') = \frac{1}{2ik_0}e^{-ik_0|x-x'|} = \frac{1}{2ik_0}e^{-ik_0 s(x-x')} \qquad (2)$$

where $s = 1$ if $x > x'$ and $s = -1$ if $x < x'$. For the incident field, we consider plane waves propagating in either the positive or negative x direction *i.e.*,

$$E^{inc}(x) = e^{-ik_0 s' x} \qquad (3)$$

where the direction of propagation is negative for $s' = -1$ and positive for $s' = 1$. Assuming a permittivity contrast which is spatially bounded to a domain $D = [x_1, x_2]$, the infinite integral in (1) collapses to D. Applying the Born approximation, namely that scattering is weak and the field within the domain D may be approximated by the incident field, (1) becomes,

$$E(x;k_0, s, s') - e^{-ik_0 s' x} = -\frac{ik_0}{2}e^{-ik_0 s x}\int_{x_1}^{x_2} \delta\varepsilon(x')e^{-ik_0(s'-s)x'}dx'. \qquad (4)$$

Above, $\delta\varepsilon(x)$ is the contrast function used to denote the unknown relative permittivity contrast $\varepsilon(x) - 1$. To solve for the unknown contrast, we begin by expanding $\delta\varepsilon(x)$ in terms of $2L$ whole-domain complex exponential basis functions,

$$\delta\varepsilon(x) \approx \sum_{l=1}^{L} a_l e^{ik_l x} + \sum_{l=1}^{L} b_l e^{-ik_l x}. \tag{5}$$

For reasons which will be made clear, the spatial frequencies are selected as $k_l = l\Delta k - \Delta k/2$, for $l = 1, \ldots, L$, where Δk is selected as $(2\pi)/(x_2 - x_1)$ *i.e.,* the fundamental wavelength is selected as twice the size of imaging domain. *The $\Delta k/2$ shift is essential as it implicitly adds a DC component into each harmonic over the imaging domain.* As a result, we eliminate the need for an explicit DC basis function.

Upon substitution of (5) into (4) we obtain a single equation in $2L$ unknowns,

$$\frac{2i}{k_0} e^{ik_0 s x}(E(x;k_0, s, s') - e^{-ik_0 s' x}) = \sum_{l=1}^{L} a_l \int_{x_1}^{x_2} e^{-i(k_0(s'-s) - k_l)x'} dx' + \sum_{l=1}^{L} b_l \int_{x_1}^{x_2} e^{-i(k_0(s'-s) + k_l)x'} dx'. \tag{6}$$

While a typical approach to obtain a system of equations from (6) would be to test, or weight the equation by means of $2L$ different inner products on the domain D [14], we must take a different approach because the domain of the left-hand side of (6) does not coincide with D. Instead, we consider $2L$ *independent* scattering experiments. Using multiple scattering experiments is a typical way of creating a sufficient number of equations [6], [9], but normally (in higher dimensions) one has the ability to construct the different scattering experiments by taking different angles of incidence, rather than different frequencies. This freedom does not exist in the 1D problem. Instead, we construct L experiments with an incident field propagating in the positive x direction where the scattering amplitude is measured at a single location $x_a < x_1$ such that $s' - s = 2$. For each of these experiments the incident field wavenumber k_0 is selected as $k_m/2$ for $m = 1, \ldots, L$. Next, we construct L experiments where the incident field propagates in the negative x direction (taking corresponding measurements at a single location $x_b > x_2$ such that $s' - s = -2$). Again we select the wavenumbers $k_0 = k_m/2$ for $m = 1, \ldots, L$. For incidence in the positive x direction we obtain the following L algebraic equations:

$$\frac{2i}{k_o} e^{-i(k_m/2)x_a}(E(x_a, k_m/2) - e^{-i(k_m/2)x_a}) = \sum_{l=1}^{L} a_l \int_{x_1}^{x_2} e^{-i(k_m - k_l)x'} dx' + \sum_{l=1}^{L} b_l \int_{x_1}^{x_2} e^{-i(k_m + k_l)x'} dx' \tag{7}$$

while for propagation in the negative x direction we obtain,

$$\frac{2i}{k_0} e^{i(k_m/2)x_b}(E(x_b;k_m/2) - e^{i(k_m/2)x_b}) = \sum_{l=1}^{L} a_l \int_{x_1}^{x_2} e^{i(k_m + k_l)x'} dx' + \sum_{l=1}^{L} b_l \int_{x_1}^{x_2} e^{i(k_m - k_l)x'} dx'. \tag{8}$$

Due to our previous choices of k_l in the expansion (5), the functions $e^{ik_m x}$ are orthogonal over the imaging domain and the combined system of equations consisting of (7) and (8) is *perfectly conditioned.* We write the system as,

$$\begin{bmatrix} \boldsymbol{I} & \boldsymbol{0} \\ \boldsymbol{0} & \boldsymbol{I} \end{bmatrix} \cdot \begin{bmatrix} \boldsymbol{a} \\ \boldsymbol{b} \end{bmatrix} = \begin{bmatrix} \boldsymbol{f} \\ \boldsymbol{g} \end{bmatrix}, \tag{9}$$

where $\boldsymbol{I}$ is the identity matrix, $\boldsymbol{a} = [a_1, a_2, \ldots, a_L]^T$ and $\boldsymbol{b} = [b_1, b_2, \ldots, b_L]^T$ are vectors of the unknown contrast expansion coefficients and $\boldsymbol{f}$ and $\boldsymbol{g}$ represent vectors of the left-hand side of (7) and (8), respectively, appropriately scaled by the width of the imaging domain. Clearly, this demonstrates that by using the proposed whole-domain basis functions and a multitude of scattering experiments we are able to produce a perfectly-conditioned system under the Born approximation. In fact, it can be shown that this result is equivalent to Fourier Imaging. Before presenting appropriate basis functions for iteratively solving the full non-linear problem, we summarize two common iterative techniques, namely the DBIM and BIM.

III. THE DISTORTED BORN ITERATIVE METHOD

The pertinent theory of the DBIM may be found in [9] and is summarized herein. As is common to many iterative techniques for solving the inverse scattering problem we consider equation (1) as two distinct equations used alternatively in a two-step updating procedure. At each iteration n, we identify from (1) the *data equation* when $x \notin D$. We assume an approximation to the fields within D (such as the Born approximation for the first iteration) and solve for the updated contrast function $\delta\varepsilon^{(n)}$. The key to the DBIM is that instead of computing $\delta\varepsilon^{(n)}$, we compute $\delta\varepsilon_b^{(n)}$

defined as the difference between $\delta\varepsilon^{(n)}$ and $\delta\varepsilon^{(n-1)}$. This is accomplished by numerically computed a Green's function $G_b^{(n-1)}$ from $\delta\varepsilon^{(n-1)}$ and the field values acquired at the $(n-1)^{th}$ iteration such that the distorted data equation becomes,

$$E(x) - E^{(n-1)}(x) = k_0^2 \int_{x_1}^{x_2} \delta\varepsilon_b^{(n)}(x') E^{(n-1)}(x') G_b^{(n-1)}(x, x') dx' \qquad x \notin D \quad (10)$$

where $E(x)$ is simply the true total field which is a measurable quantity at $x \notin D$ and $E^{(n-1)}(x)$ is the total field produced by the contrast $\delta\varepsilon^{(n-1)}$.

To compute the numerical Green's function $G_b^{(n)}$, we use,

$$G_b^{(n)}(x, x') = G(x, x') + k_0^2 \int_{x_1}^{x_2} \delta\varepsilon^{(n)}(x'') G_b^{(n)}(x'', x') G(x, x'') dx'' \quad (11)$$

where we must first solve (11) for all source points $x' \in D$ when $x \in D$. We may then use (11) with $x \notin D$ to compute $G_b^{(n)}(x, x')$ at any location in space.

Next, the *domain equation* is used to update the field within the imaging region from the updated contrast $\delta\varepsilon^{(n)} = \delta\varepsilon_b^{(n)} + \delta\varepsilon^{(n-1)}$. Formally, we consider $x \in D$ and solve

$$E^{(n)}(x) = E^{inc}(x) + k_0^2 \int_{x_1}^{x_2} \delta\varepsilon^{(n)}(x') E^{(n)}(x') G(x, x') dx'. \quad (12)$$

We may solve the full non-linear inverse problem by repeating the following procedure beginning with $n = 1$:

- Solve for $\delta\varepsilon_b^{(n)}$ from (10) using the field computed from (12) at iteration $n-1$ and update $\delta\varepsilon^{(n)}$. In the case of $n = 1$ we approximate the field using the Born approximation, hence $\delta\varepsilon^{(0)} = 0$, $E^{(0)} = E^{inc}$ and $G_b^{(0)} = G$.)

- Solve for the numerical Green's function at the observation points $x \notin D$ from equation (11) and solve for the updated field within the imaging domain from the current contrast function using (12). From the field solution within D, use (12) to directly compute $E^{(n)}$ at the observation point(s) $x \notin D$.

IV. The Born Iterative Method

While the DBIM attempts to re-use information of the profile at each iteration by formulating the problem in terms of $\delta\varepsilon_b^{(n)}$, a simpler iterative scheme that simply computes $\delta\varepsilon^{(n)}$ at each iteration without computation of the numerical Green's function may be used. This method, namely the BIM is detailed in [5]. The BIM data equation may be obtained from (10) by setting $G_b^{(n-1)}(x, x') = G(x, x')$ and $\delta\varepsilon_b^{(n)} = \delta\varepsilon^{(n)}$ for all n. Also, it is necessary to set $E^{(n-1)}(x) = E^{inc}(x)$ on the left hand side of (10). The BIM domain equation is the same as that of the DBIM.

V. An Adaptive, Whole Domain Basis formulation for the DBIM/BIM

The iterative procedure summarized in the previous section makes use of two integral equations for iteratively solving the non-linear, scalar, electromagnetic inverse scattering problem under the linearizing assumption of the Born Approximation. The domain equation (12) (which has the same form as (11)) is a second-kind integral equation and is not ill-posed. For instance it can readily be solved by expanding the unknown field quantity into pulse basis functions and using point-matching. Consequently, the solution to equations (11) and (12) will not be discussed further. Conversely, the data equation, corresponding to a linearized inverse problem, is ill-posed as discussed in Section 1 and we must either use standard regularization techniques or formulate the problem carefully. We consider therefore, the basis function expansion for the unknown contrast presented in Section 2, which, despite the ill-posedness of the problem gave an ideally conditioned matrix. It is clear however, that the orthogonality property used to produce this ideally conditioned system will vanish at subsequent iterations if the basis function expansion (5) is used. Instead, for iterations $n > 1$ in the DBIM we expand the contrast in a parameterized set of basis functions,

$$\delta\varepsilon_b^{(n)}(x) \approx \sum_{l=1}^{L} a_l^{(n)} e^{i\alpha^{(n)} k_l x} + \sum_{l=1}^{L} b_l^{(n)} e^{-i\alpha^{(n)} k_l x} \quad (13)$$

where $\alpha^{(n)}$ is an iteration dependent, real-valued parameter used to dynamically modify the basis function expansion of the unknown contrast function with the sole purpose of minimizing the condition number of the discrete matrix. (A similar expansion is used for $\delta\varepsilon^{(n)}$ in the BIM.) The motivation for minimizing the condition number of the matrix is discussed in Section 7.

Specifically, if we substitute the expansion (13) into (10), making the dependence on the measurement location and incident field direction explicit via the parameters s and s', (while dropping the explicit dependence on k_o for brevity) we obtain,

$$(E(x,s,s') - E^{(n-1)}(x,s)) = \sum_{l=1}^{L} a_l^{(n)} k_o^2 \int_{-\infty}^{\infty} e^{i\alpha^{(n)} k_l x'} E^{(n-1)}(x',s,s') G_b^{(n-1)}(x,x',s) dx' + \sum_{l=1}^{L} b_l^{(n)} k_o^2 \int_{-\infty}^{\infty} e^{-i\alpha^{(n)} k_l x'} E^{(n-1)}(x',s,s') G_b^{(n-1)}(x,x',s) dx'. \tag{14}$$

Applying the same testing procedure as the one adopted for the first-order solution we obtain an iteration dependent linear system which we write in compact form as,

$$\begin{bmatrix} \boldsymbol{E}_{11}^{(n-1)} & \boldsymbol{E}_{12}^{(n-1)} \\ \boldsymbol{E}_{21}^{(n-1)} & \boldsymbol{E}_{22}^{(n-1)} \end{bmatrix} \cdot \begin{bmatrix} \boldsymbol{a}^{(n)} \\ \boldsymbol{b}^{(n)} \end{bmatrix} = \begin{bmatrix} \boldsymbol{f}^{(n-1)} \\ \boldsymbol{g}^{(n-1)} \end{bmatrix} \tag{15}$$

where $\boldsymbol{E}_{11}^{(n-1)}$ and $\boldsymbol{E}_{21}^{(n-1)}$ are matrix representations of those terms in (14) corresponding to the coefficients $\boldsymbol{a}^{(n)}$ while $\boldsymbol{E}_{12}^{(n-1)}$ and $\boldsymbol{E}_{22}^{(n-1)}$ correspond to the terms involving $\boldsymbol{b}^{(n)}$. Equation (15) reduces to equation (10) for $n = 1$ under the Born Approximation with $\alpha^{(1)} = 1$. In the case of the BIM, the right hand side is iteration independent.

The matrix in (15) will, in general, be dense and "poorly" conditioned if the parameter $\alpha^{(n)} = 1$ is selected. Therefore, we minimize the condition number $C^{(n)}$ of the matrix by performing an optimization over the parameter $\alpha^{(n)}$. Experience has shown that the function $C^{(n)}(\alpha^{(n)})$ is not unimodal as shown in Fig. 4 and hence a global optimization routine is required and is discussed in Section 7.

VI. Extension to the BIM in 2D

In 2D the time-harmonic, lossless, non-linear, scalar inverse scattering problem for transverse magnetic (TM) fields may be mathematically represented by the 2D version of the non-linear integral equation (1),

$$E_z^{\mathrm{s}}(\vec{\rho};\vec{k}) = k_0^2 \int_{-\infty}^{\infty}\int_{-\infty}^{\infty} \delta\varepsilon(\vec{\rho}') E_z(\vec{\rho}';\vec{k}) G(\vec{\rho},\vec{\rho}';k_0) dx' dy' \tag{16}$$

where a cartesian coordinate system is assumed and the position vector is given by $\vec{\rho} = x\hat{x} + y\hat{y}$. $E_z^{\mathrm{s}}(\vec{\rho};\vec{k}) = E_z(\vec{\rho};\vec{k}) - E_z^{\mathrm{inc}}(\vec{\rho};\vec{k})$ is the z-component of the the scattered field defined as the difference between the total Field $E_z(\vec{\rho};\vec{k})$ and the incident field $E_z^{\mathrm{inc}}(\vec{\rho};\vec{k})$. The fields are parameterized by the wavevector $\vec{k} = k_x\hat{x} + k_y\hat{y}$, and the wavenumber k_0 is given by $k_0 = |\vec{k}|$. In (16), we assume the 2D, free-space Green's function $G(\vec{\rho}, \vec{\rho}';\vec{k})$,

$$G(\vec{\rho},\vec{\rho}';\vec{k}) = \frac{1}{4i} H_0^{(2)}(k_0|\vec{\rho} - \vec{\rho}'|), \tag{17}$$

where $H_0^{(2)}(x)$ is the zeroth-order Hankel function of the second kind. In the far-field, this Green's function may be replaced with its large argument approximation,

$$G(\vec{\rho},\vec{\rho}';\vec{k}) \approx \frac{i+1}{4i\sqrt{\pi}} \frac{e^{-ik_0|\vec{\rho}-\vec{\rho}'|}}{\sqrt{k_0|\vec{\rho}-\vec{\rho}'|}}. \tag{18}$$

Again, we consider incident plane waves now defined as,

$$E_z^{\mathrm{inc}}(\vec{\rho};\vec{k}) = e^{i\vec{k}\cdot\vec{\rho}}. \tag{19}$$

Under the assumption of a rectangularly bounded imaging domain $D = \{\vec{\rho}: \rho_x \in [x_1, x_2], \rho_y \in [y_1, y_2]\}$ such that the contrast function $\delta\varepsilon(\vec{\rho}) = 0 \;\; \forall\vec{\rho} \notin D$, and under the Born approximation, the integral in (16) collapses to D and becomes,

$$E_z^{\mathrm{s}}(\vec{\rho}) = \frac{k_0^2(i+1)}{4i\sqrt{\pi}\sqrt{k_0}} \int_{y_1}^{y_2}\int_{x_1}^{x_2} \delta\varepsilon(\vec{\rho}') e^{i\vec{k}\cdot\vec{\rho}'} \frac{e^{-ik_0|\vec{\rho}-\vec{\rho}'|}}{\sqrt{|\vec{\rho}-\vec{\rho}'|}} dx' dy' \tag{20}$$

where the explicit parameterization by $\vec{k}$ has been dropped for brevity. Now, making an additional far-field assumption we approximate the phase term as $|\vec{\rho} - \vec{\rho}'| \approx \rho - \hat{\rho}\cdot\vec{\rho}'$ where $\vec{\rho} = \rho\hat{\rho}$ and approximate the amplitude term by $\sqrt{|\vec{\rho}-\vec{\rho}'|} \approx \sqrt{\rho}$. Then, the integral equation becomes,

$$E_z^{\mathrm{s}}(\vec{\rho}) = \frac{k_0^2(i+1)e^{-ik_0\rho}}{4i\sqrt{\pi}\sqrt{k_0}\sqrt{\rho}} \int_{y_1}^{y_2}\int_{x_1}^{x_2} \delta\varepsilon(\vec{\rho}') e^{i\vec{k}\cdot\vec{\rho}'} e^{ik_0\hat{\rho}\cdot\vec{\rho}'} dx' dy'. \tag{21}$$

By writing the incident field wavevector $\vec{k}$ as $\vec{k} = k_0\hat{k}$ we may further reduce the integral equation to,

$$E_z^{s}(\vec{\rho}) = \beta(\vec{\rho};k_0)\int_{y_1}^{y_2}\int_{x_1}^{x_2}\delta\varepsilon(\vec{\rho}')e^{ik_0(\hat{k}+\hat{\rho})\cdot\vec{\rho}'}dx'dy' \quad (22)$$

where $\beta(\vec{\rho};k_0)$ has been used to representing the leading terms in (21). Once again, we expand the unknown contrast function in terms of whole-domain, harmonic basis functions as,

$$\delta\varepsilon(\vec{\rho}) \approx \sum_{u=-(U-1)}^{U}\sum_{v=-(V-1)}^{V} a_{u,v}e^{i((k_{xu}\hat{k}_x + k_{yv}\hat{k}_y)\cdot\vec{\rho})} \quad (23)$$

where $k_{xu} = (u-1/2)\Delta k_x$, and $k_{yv} = (v-1/2)\Delta k_y$. The coefficients $a_{u,v}$ correspond to the unknown amplitude of the $(u,v)^{\text{th}}$ basis function, while U and V limit the number of basis functions selected. For convenience we now impose a natural ordering on the pairs (u,v) such that we may re-write the basis function expansion (23) as,

$$\delta\varepsilon(\vec{\rho}) \cong \sum_{l=1}^{L} a_l e^{i(\vec{k}_l\cdot\vec{\rho})} \qquad L = 1, 2, \ldots, 4UV \quad (24)$$

where each l corresponds to a unique pair (u,v) and where $\vec{k}_l$ is given by the corresponding value $k_{xu}\hat{k}_x + k_{yv}\hat{k}_y$.

Substitution of the basis function expansion into integral equation (22) yields,

$$\frac{E_z^{s}(\vec{\rho})}{\beta(\vec{\rho};k_0)} = \sum_{l=1}^{L} a_l\int_{y_1}^{y_2}\int_{x_1}^{x_2} e^{i(\vec{k}_l\cdot\vec{\rho}')}e^{ik_0(\hat{k}+\hat{\rho})\cdot\vec{\rho}'}dx'dy'. \quad (25)$$

Thus, (25) represents a single equation in the $L = 4UV$ unknowns a_l. To obtain more equations we now considering multiple incident fields at different angles of incidence and various frequencies. Specifically, we note that if we take any incident field where $\hat{k} = \rho$, we obtain,

$$\frac{E_z^{s}(\vec{\rho})}{\beta(\vec{\rho};k_0)} = \sum_{l=1}^{L} a_l\int_{y_1}^{y_2}\int_{x_1}^{x_2} e^{i(\vec{k}_l\cdot\vec{\rho}')}e^{i(2\vec{k}\cdot\vec{\rho}')}dx'dy'. \quad (26)$$

To create a set of L equations in L unknowns we vary the incident field wavevector in a manner analogous to the 1D case *i.e.,* we let the physical wavevector $\vec{k} = \vec{k}_m/2$, for $m = 1, 2, \ldots, L$. This results in,

$$\frac{E_z^{s}(\vec{\rho}_m)}{\beta(\vec{\rho};k_m/2)} = \sum_{l=1}^{L} a_l\int_{y_1}^{y_2}\int_{x_1}^{x_2} e^{i(\vec{k}_l\cdot\vec{\rho}')}e^{i(\vec{k}_m\cdot\vec{\rho}')}dx'dy'. \quad (27)$$

where we have taken a different measurement location $\vec{\rho}_m$ for each equation. Note that $\vec{\rho}_m$ must be both in the far field, and in the direction of $\vec{k}_m$ to validate previous assumptions. Finally, we note that if we select $\Delta k_x = (2\pi)/(x_2 - x_1)$ and $\Delta k_y = (2\pi)/(y_2 - y_1)$ then the basis functions are orthogonal to the kernel of the integral operator over the domain D which reduces the inverse problem (27) to a perfectly conditioned linear system analogous to (9),

$$\boldsymbol{I}\cdot\boldsymbol{a} = \boldsymbol{f}. \quad (28)$$

Again, like the 1D case, at subsequent iterations beyond the first-order Born Approximation, we use the basis function expansion,

$$\delta\varepsilon^{(n)}(\vec{\rho}') \approx \sum_{l=1}^{L} a_l e^{i\alpha^{(n)}(\vec{k}_l\cdot\vec{\rho}')} \qquad L = 1, 2, \ldots, 4UV \quad (29)$$

where, as discussed in Sections 5, the parameter $\alpha^{(n)}$ is used to minimize the condition number of the discrete operator.

VII. Numerical Results

The iterative procedure using the adaptive basis function expansion previously described was implemented and tested. Herein we show the 1D results for a relative permittivity contrast selected to be the positive cycle of sinusoid with period 0.4 m centered over the domain $x = [-0.1, 0.1]$ having an amplitude of 2 and a rectangular contrast of amplitude 1 existing over the same domain. Data was acquired at the locations $x = -0.4$ and $x = 0.4$ m while the imaging domain was restricted to $D = [-0.3, 0.3]$ m. The contrast was expanded using 20 basis functions *i.e.* $L = 10$ and a direct search of the parameter space was performed over the range $[1, 1.4]$. The results of the 1D-DBIM and BIM are shown in Figs. 1 and 2, respectively. As expected, the DBIM method converges faster than the BIM [5], [9]. Note that in Fig. 1, the Distorted Born reconstruction for the sinusoid converges at iteration 2 and therefore, the curve for iteration 6 lies on top of the curve for iteration 2. The profile error from iteration to iteration for both methods is shown in Fig. 3 while the

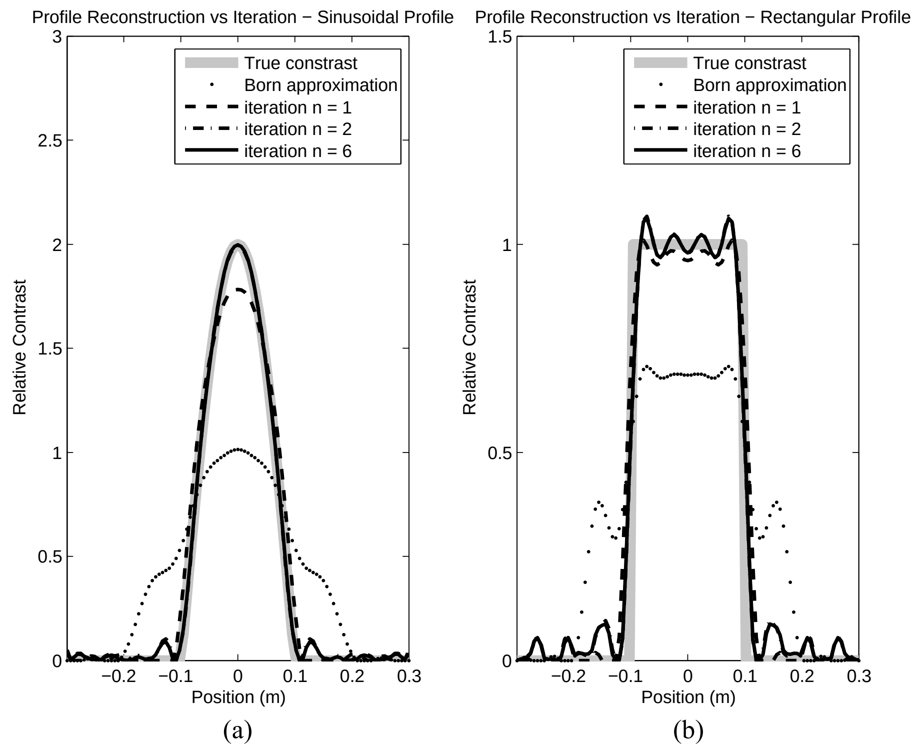

Fig. 1. 1D DBIM profile reconstruction results: sinusoidal (a), rectangular (b).

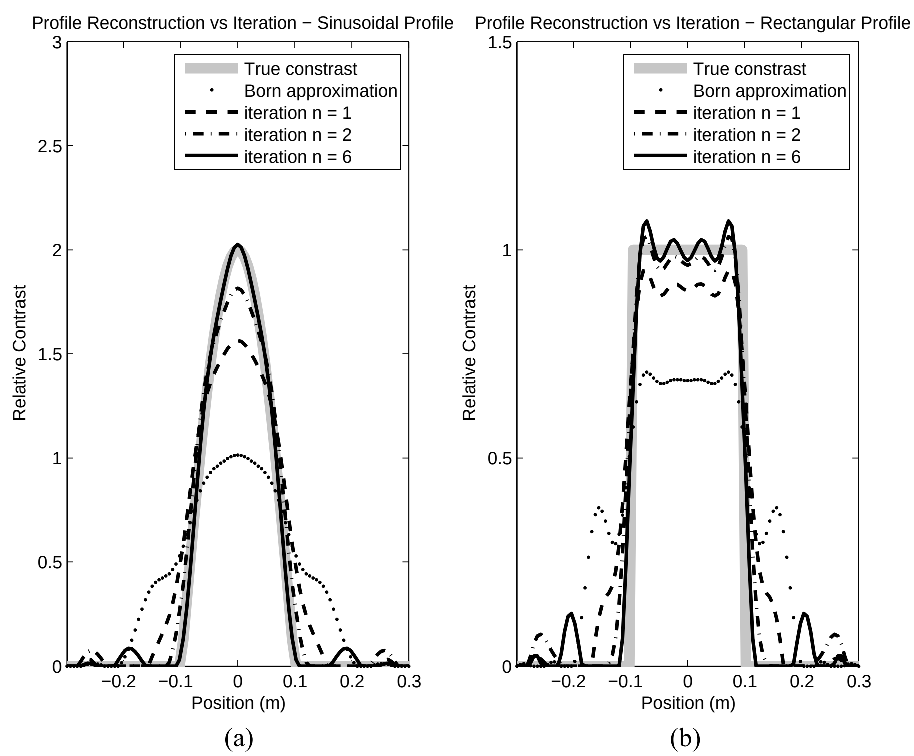

Fig. 2. 1D BIM profile reconstruction results: sinusoidal (a), rectangular (b).

system condition number versus parameter value $\alpha^{(n)}$ are shown for the two methods in Fig. 4.

For the 2D case, we show the results of the BIM for a contrast function that consists of two Gaussian pulses, centered at $(x, y) = (0.2, 0.2)$ m and $(0.3, 0.3)$ m within a square imaging domain that extends in both dimensions from 0.0 to 0.5 m. The standard deviation of each pulse is 0.025 in both spatial dimensions. The pulse closer to the origin was given a maximum amplitude of 2 while the other, an amplitude of 1. To iteratively reproduce the contrasts we used 144 basis functions (selecting $U = V = 6$). Figure 5 shows the true contrast function and reconstructed profiles after the Born approximation and the sixth iteration.

In all cases, the forward solution was obtained from a MoM formulation using a pulse basis over the imaging domain.

VIII. Discussion

While a rigorous mathematical investigation of the effects of our parameterized basis function expansion is subject to ongoing research, we can suggest three immediate reasons why this technique is a good candidate for solving the linearized inverse scattering problem. First, the very nature of the basis function expansion limits the high frequency components of the reconstructed profile which, as discussed in Section 1, contributes to the ill-posedness of the original problem. Second, as the condition number is defined as the ratio of the largest to smallest singular values of the operator matrix, we are implicitly demanding that the solution to the discrete system, corresponding to the basis function coefficients, is not overwhelmed by unconstrained high frequencies. This can be seen by ordering the singular

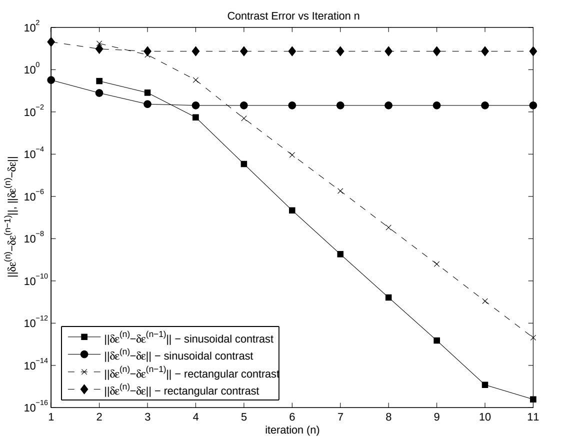

(a)

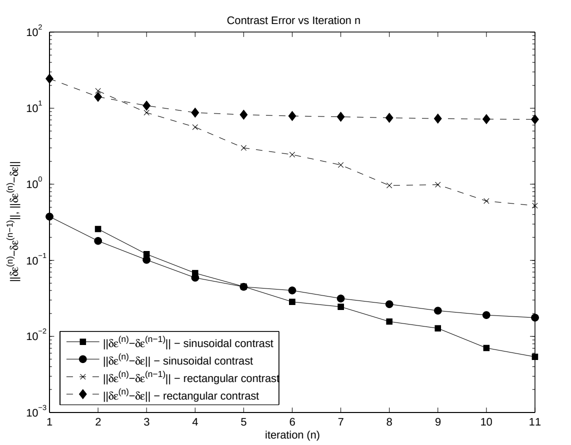

(b)

Fig. 3. 1D error convergence: DBIM (a), BIM (b). The values corresponding to the rectangular contrast have been increased by a factor of 100 for clarity.

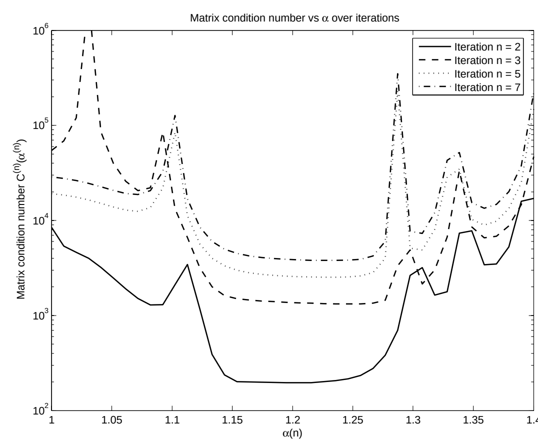

(a)

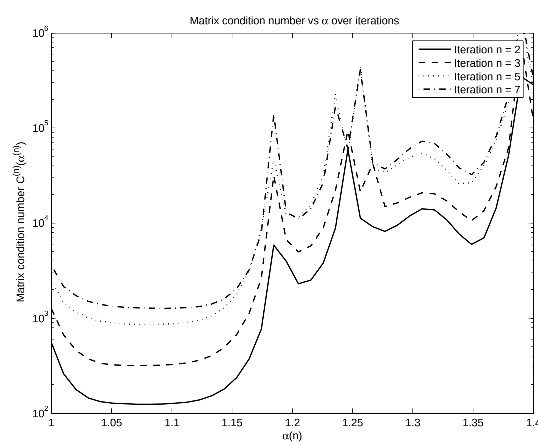

(b)

Fig. 4. 1D condition number as a function of $\alpha^{(n)}$ for various iterations: DBIM (a), BIM (b). Condition number values have been increased by a factor of 10 times the iteration count for clarity.

values of the discrete operator in non-increasing order and noting that the corresponding singular vectors have a non-decreasing number of zero crossings. frequency [4]. Lastly, and perhaps most importantly, if we consider the multiple-frequency approach in conjunction with minimization of the condition number as a sort of regularization technique itself, the selection of the basis function parameter (which, in this context would double as the regularization parameter) is well-defined: we select the value of the regularization parameter which minimizes the condition number of the discrete operator.

Two comments should be made. First, at an arbitrary iteration n, the function $C^{(n)}(\alpha^{(n)})$ is not unimodal and an optimization technique is required to determine the optimal value of $\alpha^{(n)}$. For the results shown in this paper, as the optimization space is over a single parameter (for both the 1D and 2D formulations), we have used a direct search over the parameter space. Empirically, we have found that at each iteration, the condition number has a global minimum on the interval $\alpha^{(n)} \in [1, \alpha^{(n)}_{\max}]$ where,

$$\alpha^{(n)}_{\max} = \sqrt{\max(\mathrm{Re}(\delta\varepsilon^{(n)}(x)) + 1)}\,. \tag{30}$$

The previous expression is motivated by the fact that the basis function parameter is present as a phase term in the basis function expansion and should therefore be in some way proportional to the field velocity in the medium. Fig. 4 shows typical behaviour of the condition number as a function of the regularization parameter.

Clearly, minimizing the condition number of the matrix involves the repetitive computation of the discrete operator for each $\alpha^{(n)} \in [1, \alpha^{(n)}_{\max}]$ and its condition number. Fortunately, the number of harmonic basis functions required to satisfactorily reproduce an unknown contrast function is generally much less than if a pulse basis expansion was considered. As a result, the condition number evaluation does not pose significant computational strain.

Second, in many cases the condition number of the operator matrix is not unreasonably large. Nevertheless, minimization of the condition number is *still required* to obtain a good solution. Thus, at each iteration, it is essential to pick $\alpha^{(n)}$ corresponding to the *minimal* condition number and not to one that appears "sufficiently small".

IX. CONCLUSIONS

Herein we have shown that it is possible to avoid the use of common regularization techniques in the iterative solution to the inverse scattering problem by carefully formulating the experiments used to construct the discrete linearized inverse problem. Specifically, adopting a multiple-frequency formulation with adaptive

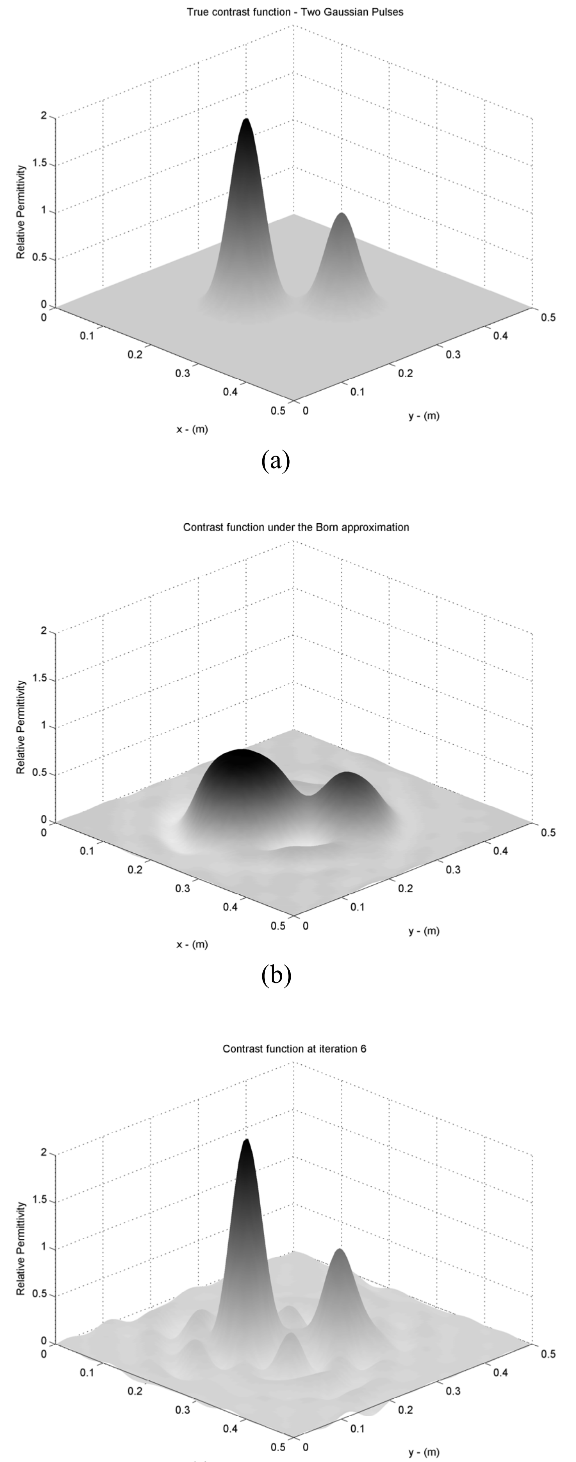

Fig. 5. 2D BIM profile reconstruction results: True contrast (a), first-order (b), and after six iterations (c).

basis functions and a global optimization over the basis parameter provides a well-conditioned matrix at each iteration. We have demonstrated the applicability of our adaptive basis functions to both the DBIM and BIM methods in 1D as well as to the BIM method in 2D (application to the 2D DBIM method poses no theoretical problems). Our current concerns are convergence to high-contrast profiles but this seems to be a problem which may be inherent in the Iterative Born techniques [2]. Even if this is the case, we plan on applying our approach of properly formulating the problem to other (possibly non-iterative) solution methods in order to determine exactly in what cases the usual regularization methods are avoidable. Future work will include a rigorous analysis of the ability of the proposed basis functions to reconstruct profiles in the presence of noisy field data. Also, we will consider an analysis for an optimum number of basis functions at each iteration.

ACKNOWLEDGEMENTS

The authors would like to acknowledge NSERC for supporting this research.

REFERENCES

[1] W. C. Chew, *Waves and Fields in Inhomogeneous Media*, IEEE Press, 1990.

[2] M. Oristaglio and H. Blok, “Wavefield Imaging and Inversion in Electromagnetics and Acoustics,” *lecture notes,* Delft University, 2000.

[3] M. Born and E. Wolf, *Principles of Optics*, 7th~ed, Cambridge University Press, 1999.

[4] P. C. Hansen, “Numerical tools for analysis and solution of Fredholm integral equations of the first kind,” *Inverse Problems* vol. 8, pp. 849-872, 1992.

[5] Y. M. Wang and W. C. Chew, “An iterative solution of two-dimensional electromagnetic inverse scattering problem,” *Int. J. Imaging Syst. Technol.*, vol. 1, no. 1, pp. 100-108, 1989.

[6] Q. H. Liu *et. al.*, “Active Microwave Imaging I - 2-D Forward and Inverse Scattering Methods”, *IEEE Trans. Micro. Theo. and Tech.*, vol. 50, no. 1, pp. 123-133, 2002.

[7] F. Soldovieri and R. Persico, “Reconstruction of an Embedded Slab from Multifrequency Scattered Field Data Under the Distroted Born Approximation,” *IEEE Trans. Ant. and Propagat.*, vol. 52, no. 9, pp. 2348-2356, 2004.

[8] A. J. Devaney, “Nonuniqueness in the inverse scattering problem,” *J. Math. Phs.*, vol. 19, no. 7, pp. 1526-1531, 1978.

[9] W. C. Chew and Y. M. Wang, “Reconstruction of two-dimensional permittivity distribution using the distorted born iterative method,” *IEEE Trans. Med. Imag.*, vol. 9, pp. 218–25, June 1990.

[10] V. I. Okhmatovski and J. LoVetri, “A Well-Conditioned Formulation of 1D Inverse Scattering Problem Under the Born Approximation,” *ANTEM*, 2005.

[11] I. Jeffrey, V. I. Okhmatovski, and J. LoVetri, “A Well-Conditioned Solution to the 1D Inverse Scattering Problem using the Distorted Born Iterative Method,” *ACES 2006,* Miami Florida, 2006.

[12] I. Jeffrey, V. I. Okhmatovski, and J. LoVetri, “A Modified Well-Conditioned Iterative Solution to the 1D Inverse Scattering Problem using the Born Iterative Method,” *IEEE AP-S 2006*, Albuquerque, New Mexico, 2006.

[13] C. Gilmore, I. Jeffrey, V. I. Okhmatovski, and J. LoVetri, “A Novel Multi-Frequency Regularization Method for the 2D Inverse Scattering Problem,” *ANTEM 2006,* Montreal, Quebec, 2006.

[14] R. F. Harrington, *Field Computation by Moment Methods*, New York: Maxmillan, 1968.

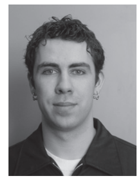

Ian Jeffrey received the B.Sc degree in Computer Engineering (with distinction) in 2002 and the M.Sc degree in Electrical and Computer Engineering in 2004 from the University of Manitoba, Winnipeg, Canada where he is currently working towards the Ph.D Degree in Electrical and Computer Engineering. His current research interests are in fast algorithms for computational electromagnetics, electromagnetic compatibility and inverse problems. Mr. Jeffrey held a Canadian NSERC Post-Graduate Scholarship A from 2002-2004 and currently holds an NSERC Post-Graduate Scholarship B.

Vladimir I. Okhmatovski was born in Moscow, Russia, in 1974. He received the M.S. (with distinction) and Candidate of Science (Ph.D.) degrees from the Moscow Power Engineering Institute, Russia, in 1996 and 1997, respectively. In 1997, he joined the Radio Engineering Department, Moscow Power Engineering Institute, as an Assistant Professor. From 1998 to 1999, he was a Post-Doctoral Research Associate with the National Technical University of Athens. From 1999 to 2003, he was a Post-Doctoral Research Associate with the University of Illinois at Urbana-Champaign. From 2003 to 2004, he was with the Department of Custom Integrated Circuits Advanced Research and Development, Cadence Design Systems Inc. He is currently an Assistant Professor with the Department of Electrical and Computer Engineering, University of Manitoba, Winnipeg, MB, Canada. His research interests are the fast algorithms of computational electromagnetics and modeling of high-speed digital circuits and mixed-signal components.

Joe LoVetri received the Ph.D. degree in electrical engineering from the University of Ottawa, ON, Canada, in 1991. From 1991 to 1999, he was an Associate Professor in the Department of Electrical and Computer Engineering, The University of Western Ontario, London, Ontario, Canada. He is currently a Professor in the Department of Electrical and Computer Engineering, and Associate Dean (Research) of the Faculty of Engineering, at University of Manitoba, Winnipeg, Canada. His main research interests are in time-domain CEM, modeling of EMC problems, GPR, and inverse imaging techniques.

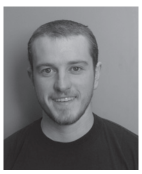

Colin Gilmore received the B.Sc degree in Electrical Engineering (with distinction and winning the gold medal) in 2002 and the M.Sc Degree in Electrical Engineering in 2005 both from the University of Manitoba, Winnipeg, Canada where he is currently working towards the Ph.D Degree in Electrical Engineering. His current research interests are in the areas of GPR, signal processing, computational electromagnetics and inverse problems. Mr. Gilmore held a Canadian Natural Sciences and Engineering Research Council (NSERC) Post-Graduate Scholarship A from 2002-2004 and currently holds an NSERC Canada Graduate Scholarship.